Chromatin Changes in Cell Transformation: Progressive Unfolding of the Higher-Order Structure during the Evolution of Rat Hepatocyte Nodules. A Differential Scanning Calorimetry Study

Paola Barboro,*Andrea Pasini,* Silvio Parodi,* Cecilia Balbi,* Barbara Cavazza,‡ Caterina Allera,‡
Giuseppe Lazzarini,‡ and Eligio Patrone‡

*Istituto Nazionale per la Ricerca sul Cancro and ‡Centro di Studi Chimico-Fisici di Macromolecole Sintetiche e Naturali, Genoa, Italy

ABSTRACT   Using differential scanning calorimetry and complementary ultrastructural observations, we have characterized the status of chromatin during the transformation of rat hepatocytes in the resistant hepatocyte model of Solt and Farber (1976. *Nature (Lond.)*. 263:701–703). Differential scanning calorimetry affords a measure of the degree of condensation of chromatin in situ and has therefore been used in this work for the purpose of establishing the nature of the structural changes associated with the emergence of successive cellular populations. Since the resistant hepatocyte model generates a series of synchronous phenotypic changes, it was possible to determine unambiguously the content of heterochromatin at each step of the process.

The higher-order structure undergoes a partial relaxation in early developing nodules, isolated 16 weeks after initiation; the thermal transition at 90°C, which is characteristic of noninteracting core particles, increases with respect to control hepatocytes. Dramatic changes occurr in persistent (46-week) nodules. The 90°C endotherm dominates the thermogram, while the transition at 107°C, corresponding to the denaturation of the core particle packaged within the heterochromatic domains, disappears. The complete loss of the higher-order structure at this stage of transformation has been further verified by ultrastructural observations on thin nuclear sections. Ten-nm filaments, having a beaded appearance, are scattered throughout the nucleoplasm and clearly result from the decondensation of 30-nm-thick fibers. This catastrophic relaxation process cannot be related to an effective increase in gene activity. Rather, our observations suggest that during transformation chromatin is in a state of high transcriptional competence associated with the alert of general cellular programs. This view is consistent with the finding that in persistent nodules the DNA is extensively hypomethylated with respect to normal liver.

INTRODUCTION

From its inception, the concept of the pivotal role of chromatin structure in gene regulation has aroused a great deal of interest. The observation of thin nuclear sections in the electron microscope, in combination with harsh fractionation techniques, has been used to demonstrate that most of the nuclear RNA is associated with the loose, soluble chromatin fraction, while the condensed (heterochromatic) regions are in a transcriptionally inactive state (Frenster, 1974). The somewhat naïve statement that unfolded and condensed domains of the genome are sharply differentiated at the functional level has provided, over the past several years, the impetus to learn more about the structural changes of chromatin underlying gene activation (Weintraub, 1985). A critical examination of this view requires, however, that two issues be recognized. The first is the necessity of defining the molecular events relating to transcription. Our knowledge of the changes in chromatin structure and nucleosome positioning associated with the transcriptional activity of some genes is increasing steadily (Weisbrod, 1982; Villeponteau et al., 1992). The second is the question of whether heterochromatin formation is involved in permanently turning off

a given set of genes. Although this possibility was suggested several years ago (Weintraub, 1985), it has received very little attention because of the difficulty in envisaging clear-cut supporting experiments. Moreover, theoretical models which assume that the structure of inert genes consists of an extended array of nucleosomes have been developed (Svaren and Chalkley, 1990). That is to say, higher-order folding plays no functional role.

However, a dramatically different picture is emerging from a series of recent investigations on the genetics of position-effect variegation in *Drosophila* (Dorn et al., 1986; Reuter et al., 1990). Heterochromatic inactivation occurs whenever a chromosome rearrangement places the gene near a heterochromatin domain. The repression depends on changes in the physical state of the chromatin surrounding the gene, which undergoes an extensive condensation process. The most compelling outcome of this research up to the present has been the identification of a few modulating factors of variegation, for example, a zinc-finger protein that acts as an enhancer of heterochromatin formation (Reuter et al., 1990). Furthermore, the dominant mutation su-(var)21[0,1], which suppresses position-effect variegation, results in an increase in the acetylation of histone H4 (Dorn et al., 1986). Undoubtedly, the peculiar architecture of the polythene chromosome represents a major advantage, since it allows direct observation of the structural changes occurring around the variegating locus. Excluding the Barr body, no definite heterochromatic pattern can be

recognized within the mammalian nucleus by current observation methods. Even the best electron micrographs of thin nuclear sections show nothing but the local unraveling of electron-opaque, 30-nm threads (Olins and Olins, 1979).

A few years ago, we tackled the problem of developing new experimental methods suitable for analyzing the structure of chromatin in situ. Previous work from different laboratories (Staynov, 1976; Weischet et al., 1978) had already demonstrated that, in the case of both chromatin and isolated core particles at low ionic strength, the derivative of the hyperchromicity curve at 260 nm as a function of the temperature reveals several thermal transitions, each transition corresponding to the unstacking of an energetically distinguishable domain of nucleosomal DNA. We wondered whether information on the higher-order structure of native chromatin could be obtained by differential scanning calorimetry (DSC) of carefully isolated nuclei. The calorimetric approach turned out to be strikingly successful (Nicolini et al., 1983; Balbi et al., 1988, 1989; Cavazza et al., 1991). Condensation-decondensation phenomena of chromatin can be directly monitored in situ by DSC of isolated nuclei, and the amount of heterochromatin can be quantitatively determined. A concise account of the principles and applications of the method will be given in this paper, by commenting on the thermal profiles of nuclei from different sources.

Two major experimental models for establishing the general function of heterochromatin in eukaryotic gene regulation are available. The recognition of the pattern of heterochromatin formation during early embryonic development could provide a direct answer. Unfortunately such a crucial investigation involves enormous experimental difficulties, especially if physicochemical methods are employed. Likewise, the process of transformation entails changes in the cellular program that are propagated to daughter cells and therefore lends itself to a systematic analysis of the chromatin changes. Of course, for a transformation model to be useful, the new cellular populations must emerge in a synchronous fashion.

The resistant hepatocyte model for liver carcinogenesis (Solt and Farber, 1976) represents the best tool available for investigating the multistep development of cancer. Within 4 weeks after initiation, early nodules develop by clonal expansion of each rare resistant hepatocyte. After a few weeks the majority redifferentiate back to normal liver. The subsequent cellular population (persistent nodules), however, undergoes a progressive evolution culminating in the onset of cancer. Very little is known about the biochemical and morphological changes occurring at this stage. Since early and persistent nodules develop in an orderly fashion, homogeneous preparations can be easily obtained by carrying out the isolation at the appropriate time after initiation. Therefore, it is possible to unambiguously analyze the status of heterochromatin at each stage of transformation. The results reported in this paper demonstrate that the heterochromatin content decreases in early nodules compared to normal

tissue. This process reaches its height with complete decondensation in persistent nodules.

MATERIALS AND METHODS

Induction of hepatocyte nodules

Nodules were induced by the procedure of Solt and Farber as modified by Semple-Roberts et al. (1987). Briefly, male Fisher F-344 rats (Charles River, Como, Italy) weighing 100–130 g were initiated with 200 mg/kg of diethylnitrosoamine; 2 weeks later 2-acetylaminofluorene, at a dose of 20 mg/kg/day, was administred by gavage on 3 consecutive days followed by partial hepatectomy. Finally, 5 days later a single dose of 2-acetylaminofluorene (5 mg/kg) was administered. The number and size of nodules were determined by hematoxylin-eosin and γ-glutamyl transpeptidase staining.

Cell culture

The cell lines used in this investigation were epithelial cells derived from normal and benzo-α-pyrene-treated rat lung (referred to here as TE and BPE, respectively). They were obtained from the laboratory of I. Chouroulinkow (Institut de Recherches Scientifiques sur le Cancer, CNRS, Villejuif, France). The cells were cultured at 37°C in Dulbecco's modified Eagle's medium supplemented with 10% fetal bovine serum in a humidified atmosphere of 5% CO_2. The cells were grown to a density of 20×10^6 cells/150 cm^2 tissue culture flask. The culture medium was removed, and the cells were washed in dissociation medium (DM) consisting of 75 mM NaCl and 24 mM Na_2EDTA (pH 7.8), harvested with a rubber policemen, and resuspended in DM at a concentration of 1×10^6 cells/ml.

Isolation of nuclei

The animals were fasted 24 h before sacrifice and anesthetized with penthotal (50 mg/kg), and the liver was perfused in situ as previously described (Parodi et al., 1983), except that the Merchant's solution contained 5 mM $Na_2S_2O_5$ and 1 mM phenylmethylsulfonyl fluoride. All the preparative steps were carried out at 4°C; in addition to phenylmethylsulfonyl fluoride and $Na_2S_2O_5$ the buffers were supplemented with a mixture of proteases inhibitors (20 μg/ml leupeptin, 25 μg/ml aprotinin, 10 μg/ml pepstatin, 0.5 mM benzamide) according to the method of Tokés and Clawson (1989); all the inhibitors were purchased from Sigma Chimica (Milan, Italy). The liver was excised, and control tissue or isolated nodules were minced in 20 ml of DM. After gentle homogenization in a loose-fitting potter and sieving through a stainless steel grid, hepatocytes were harvested by centrifugation at $150 \times g$ for 4 min. As a consequence of both the low centrifugal force and the shortness of the sedimentation time, this procedure yielded an almost homogeneous preparation of hepatocytes (parenchymal cells), as judged from observations with a light microscope equipped with phase-contrast optics. The pellet was resuspended in DM at a concentration of 1×10^6 cells/ml and nuclei isolated by a continuous extraction procedure in the presence of Triton X-100, as already described (Balbi et al., 1989). This protocol yields very stable nuclear preparations (Balbi et al., 1989) containing residual cytoskeletal proteins as major contaminations, as judged from the electrophoretic pattern of total nuclear proteins on 8–15% gradient sodium dodecyl sulfate (SDS)-polyacrylamide gels (Cavazza et al., 1991); only actin and two intermediate filament proteins, cytokeratins A and D (Franke et al., 1981), copurify with the nucleus (for a representative electropherogram see the inset in Fig. 1 a). Nuclei from cultured cells were obtained in the same manner. The preparation of calf thymus nuclei from frozen tissue was carried out as reported previously (Cavazza et al., 1991).

Calorimetric measurements

Nuclei were resuspended in DM and centrifuged at $10,000 \times g$ for 15 min. The pellet was transferred into large-volume (75 μl) calorimetric capsules.

FIGURE 1 (a) comparison among the thermal profiles of nuclei isolated from mature tissues and actively dividing cells. Scan 1, rat liver; scan 2, calf thymus; scans 3 and 4, TE and BPE cell lines, respectively. The main endotherms, arising from the denaturation of the DNA domains in chromatin, are marked with Roman numerals. The amount of DNA in each sample of nuclei was 0.8 mg (rat liver), 2.6 mg (calf thymus), 0.68 mg (TE cells), and 1.13 mg (BPE cells). (b) decondensation of calf thymus chromatin at low ionic strength. This experiments mimics the major features of the unfolding process occurring in vivo. Calf thymus nuclei were equilibrated with dilute DM (Na$^+$ concentration, 10 mM) at 25°C, and aliquots of the pellet were scanned at different times from equilibration. Scan 1, native nuclei in DM. Scans 2 and 3 correspond to 15- and 30-min incubations, respectively, in the low-salt buffer. The amount of DNA was 3.2, 3.49, and 1.7 mg (scans 1, 2, and 3, respectively). (Inset) electrophoretic characterization of total nuclear proteins from control rat hepatocytes on 8–15% gradient SDS-polyacrylamide gels. Note that only actin (Ac) and the major cytokeratins of rat liver (CKA and CKD) are co-isolated in appreciable amounts with the nucleus. Histone H1 and core histones are designated by H1 and CH, respectively. The molecular weight of standard proteins ($\times 10^{-3}$) appears on the left.
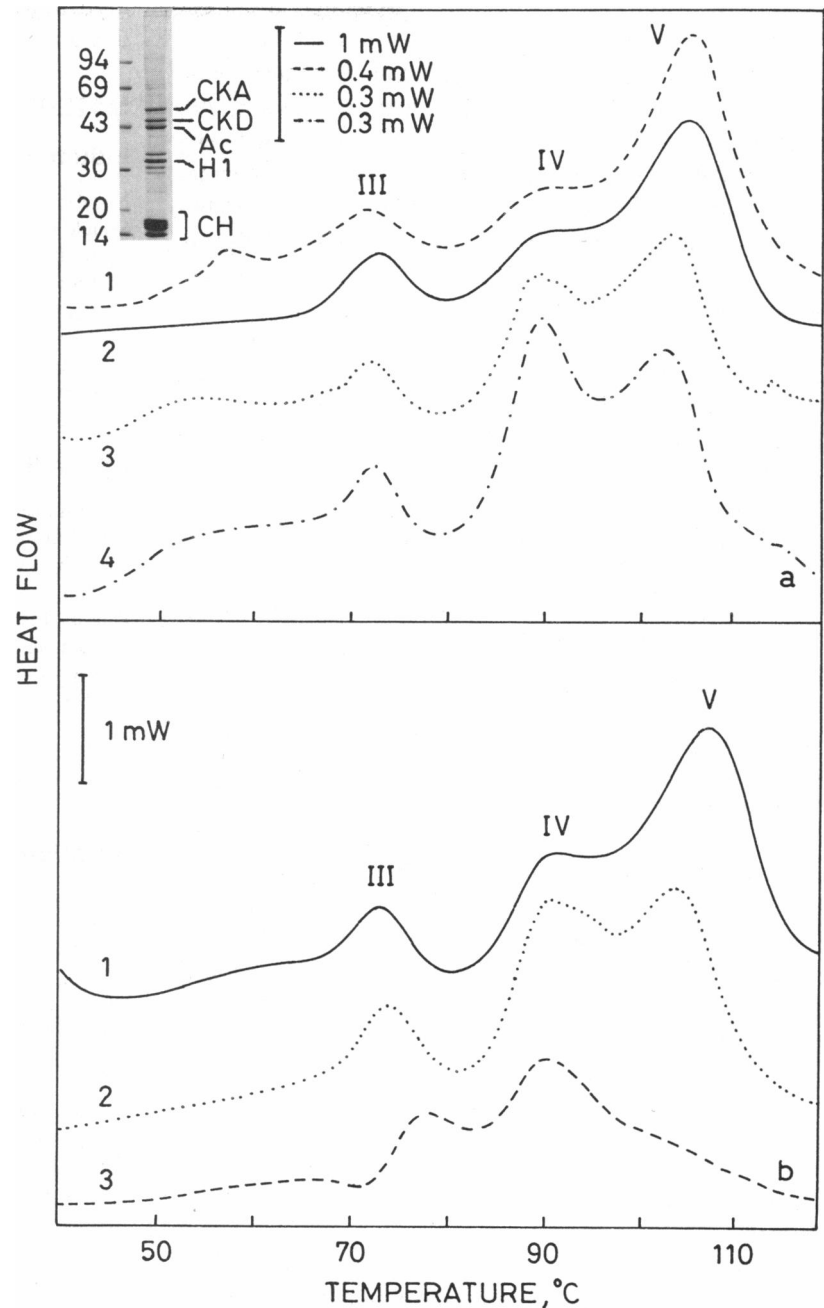
Measurements were performed with a Perkin-Elmer DSC7 (Perkin-Elmer Corporation, Norwalk, CT) from 10°C to 125°C at a scanning rate of 10°C/min. The samples used in the experiments contained from ~0.1 to 3.5 mg of DNA, depending on the tissue or cell line analyzed. Deconvolution of the excess heat capacity curves was performed as already reported (Cavazza et al., 1991).

Electron microscopy

Fixation, embedding, and sectioning of hepatocytes for electron microscopy were performed according to standard techniques. About 2×10^7 cells were resuspended in 1 ml of DM, pelleted by centrifugation at 2000 $\times g$ for 15 min, and washed three times in a solution containing 100 mM NaCl, 10 mM Tris-HCl (pH 7.5), 1 mM Na$_2$EDTA, and 1 mM EGTA. The pellet was fixed in 2.5% glutaraldehyde in 100 mM NaCl and 10 mM Tris-HCl (pH 7.5) for 2 h at 4°C and postfixed in OsO$_4$ in phosphate buffer (pH 7.2) for 1 h. Following dehydratation in ethanol, the samples

were embedded in Durcupan (Fluka, Buchs, Switzerland). Thin sections were obtained with a Reichert OmU2 (Reichert, Vienna, Austria) ultramicrotome equipped with a diamond knife. Sections giving a gray to silver interference color were mounted on uncoated nickel grids, stained with 4% uranyl acetate in 50% ethanol, counterstained with 0.4% aqueous lead citrate, brought to pH 12.5 with concentrated NaOH, and examined with a Siemens 102 electron microscope (Siemens, Karlsruhe, Germany) operating at 80 kV.

Other methods

The chemical assay of DNA, RNA, and proteins as well as the electrophoresis of DNA and of total nuclear proteins on 0.6% agarose and 8–15% gradient SDS-polyacrylamide gels, respectively, were performed as already reported (Balbi et al., 1989; Cavazza et al., 1991). In vitro decondensation of nuclear chromatin at low ionic strength was carried out exactly as described in a previous paper (Cavazza et al., 1991).

RESULTS

DSC profile of isolated nuclei reflects the status of chromatin in situ. Experimental results and fundamentals of the calorimetric method

Early in our exploratory study it became apparent that the DSC profile of isolated nuclei holds direct information on the fraction of nucleosomes packaged within condensed (heterochromatic) domains. Consider the raw data reported in Fig. 1 a, relative to nuclei isolated from both mature tissues (scans 1 and 2) and rapidly dividing cells (scans 3 and 4). For the sake of an immediate appreciation of the results the deconvolution of the thermograms into component thermal transitions has not been reported; an estimate of the fraction of denaturation heat absorbed in each endotherm is obtained on visual inspection of the scans.

As a rule, in the case of nuclei isolated by the continuous (in flow) extraction procedure only small thermal effects are observed between 50 and 70°C; the unfolding of residual cytoskeletal filaments, nuclear matrix, and histones occurs within this temperature range (Balbi et al., 1989; Cavazza et al., 1991). Three major endotherms, marked with Roman numerals, reflect the unstacking of nuclear DNA and are consistently observed at 75, 90, and 107°C (endotherms III, IV, and V), irrespective of the cell type. In contrast to the steadiness of the transition temperature (T_m), however, significant differences in the denaturation heat are apparent. In the case of rat liver and calf thymus (scans 1 and 2) transition V dominates the thermogram. A comparable situation is observed for rapidly dividing TE cells, although an increase in the heat absorbed around 100°C is also apparent (scan 3). Dramatic differences in the DSC profile are seen, however, in the case of BPE cells. The major heat investment occurs in endotherm IV (scan 4). These results suggest that the DSC profile can be used to distinguish between resting and dividing cells and, more importantly, that the increase in the transition enthalpy at 90°C ($\Delta H_m{}^{IV}$) reveals changes in the physical state of chromatin relating to transformation.

Following our early DSC experiments (Nicolini et al., 1983) Cole and his co-workers have reported several interesting observations on the increase in $\Delta H_m{}^{IV}$ that occurs during differentiation of mouse neuroblastoma cells (Touchette et al., 1986) as well as in the course of aging of human fibroblasts (Almagor and Cole, 1989). In interpreting their data, these authors suggested that endotherm IV corresponds to the unstacking of relaxed DNA, whereas the melting of DNA or chromatin constrained in a loop gives rise to endotherm V. Undoubtedly, this contention is consistent with the finding that the latter transition is lost when nuclei are digested with micrococcal nuclease or DNAse I (Balbi et al., 1989; Touchette and Cole, 1985). The results of recent investigations from our laboratory on the structural changes of nuclear chromatin, using different physicochemical techniques and electron microscopy in combination with DSC, led to the definitive assignment of each transition (Balbi et al., 1989; Cavazza et al., 1991). The detection of the struc-

tural elements of chromatin by DSC rests on the sharp subdivision of the polynucleosomal chain into energetically distinguishable domains, which in turn results from the tight binding of 150 base pairs of DNA to the histone octamer. The unprotected DNA segment, the linker, melts in transition III (see Fig. 1), whereas the denaturation of the core particle DNA occurs, when the polynucleosomal chain assumes the unfolded conformation, in endotherm IV at 90°C (Balbi et al., 1989). These attributions are consistent with previous investigations on the optical melting of isolated chromatin at low ionic strength (Fulmer and Fasman, 1979), as demonstrated by the extrapolation of the denaturation temperatures of the nucleosomal domains, plotted against the logarithm of the counter-ion concentration, to physiological ionic strength (Balbi et al., 1989), and have been further verified by analyzing the temperature dependence of the infrared spectrum of calf thymus nuclei in the 1300–1800 cm^{-1} region (Cavazza et al., 1991). Endotherm V at 107°C was found to arise from the denaturation of core particle DNA when the core particles interact in an orderly fashion within the higher-order (condensed) structure. Its actual relation to transition IV has been established by ethidium intercalation and micrococcal nuclease digestion experiments (Balbi et al., 1988, 1989) as well as by submitting nuclear chromatin to a cyclic change of the ionic strength (Cavazza et al., 1991); the transition between the folded and the unfolded states results in an abrupt conversion of transition V into transition IV and vice versa.

Several physical and chemical methods can be used to condense (or decondense) chromatin at equilibrium. They include the manipulation of ionic strength (Cavazza et al., 1991), the use of intercalating agents (Balbi et al., 1988) and the DNA-binding drug distamycin (C. Balbi, unpublished results). Perhaps the superb capability of DSC techniques to detect the structural changes of chromatin in situ has been best demonstrated by investigating the dependence of the high-temperature region of the thermal profile on the ionic conditions; the data shown in Fig. 1 b are relative to calf thymus nuclei decondensed in dilute DM (Na^+ concentration, 10 mM) at 25°C, according to a standard procedure (Cavazza et al., 1991). After a 15-min incubation, the dominance of transition V characteristic of the native material (scan 1) is lost; $\Delta H_m{}^{IV}$ is approximately equal to $\Delta H_m{}^{V}$ (scan 2). Complete decondensation is achieved after 30 min (scan 3). Leaving the kinetic aspects out of consideration, the thermodynamic analysis of the calorimetric data shows that the transition is an athermal process; that is, there is no enthalpic contribution in the Gibbs free energy of condensation. In fact, the total denaturation enthalpy of chromatin remains constant in the course of the conformation change; the equilibrium increase (or decrease) in the enthalpy at 107°C is quantitatively compensated by an opposite change at 90°C (Cavazza et al., 1991). Therefore, the ratio $\Delta H_m{}^{V}/(\Delta H_m{}^{IV} + \Delta H_m{}^{V})$ represents a measure of the average degree of condensation, a useful parameter for characterizing the status of nuclear chromatin.

Calorimetric behavior of early and persistent nodules

In Fig. 2 we show the high-temperature region of the thermograms of early developing (a) and persistent (b) nodules, isolated 16 and 46 weeks after initiation, respectively. Since nodules represent only a small fraction of the liver weight, in these experiments the amount of DNA scanned in the calorimeter was on the average 0.3 mg, which is much less than that used in the case of normal tissue or cell cultures. This circumstance worsens somewhat the signal-to-noise ratio, but the relevant enthalpy changes that occur beyond 80°C can still be measured with reasonable accurancy (limits of the SD ± 15%). Progressive, extensive decondensation occurs during the evolution of normal hepatocytes (Fig. 1 a, scan 1)
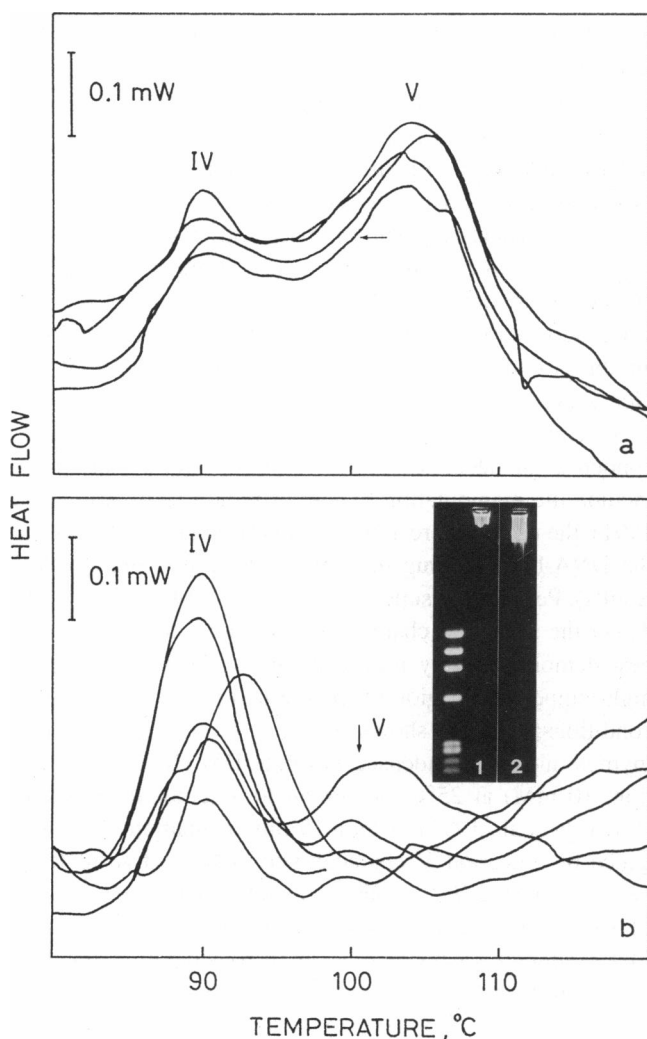

FIGURE 2 The thermograms of nuclei isolated from different preparations of (a) early developing (16-week) and (b) persistent (46-week) nodules. The main endotherms, arising from the denaturation of core particle DNA, are marked with Roman numerals. The deconvolution of the thermogram marked with an arrow in (a) is reported in Fig. 3 b. Differences in the area under the thermal profiles depend on the variability of the size of samples, which contained from 0.34 to 0.48 (a) and from 0.1 to 0.3 (b) mg of DNA. The inset in (b) shows the 0.6% agarose gel electrophoresis of the DNA isolated from control hepatpcytes (lane 1) and persistent nodules (lane 2). The molecular weight marker is HaeIII digest of ϕX174 DNA.

to persistent nodules (Fig. 2 b). The thermal profile of the latter shows nothing but a dominant, sharply defined endotherm at 90.4 ± 1.2°C (mean of six determinations ± SD), with a residual thermal effect around 100°C, which is as a rule too small to be measured accurately and approximately accounts for 10% of the total transition enthalpy of core particle DNA; in only one experiment out of six (marked with an arrow in Fig. 2 b) has a value of about 40% been obtained. This melting behavior is characteristic of the polynucleosomal chain in the unfolded conformation, as exemplified by the decondensation of calf thymus chromatin at low ionic strength, which has been commented on in the previous section. Early developing nodules (Fig. 2 a) are in an intermediate state, since the enthalpy at 90°C increases with respect to the control, while the endotherm at 107°C decreases and broadens toward lower temperatures.

Before we comment on the ultrastructural changes of chromatin in nodules, we recall a few, well-established features of the conformational changes of the polynucleosomal chain occurring in vitro, which are believed to mimic the mechanism of unfolding and refolding operating in vivo. The terms "higher-order structure" and "condensed state" are currently used as synonyms, since the folding of the 10-nm filament involves as the major step the ordered packaging of nucleosomes in a contact helix (the 30-nm fiber, or solenoid), as shown by the appearance of low-angle x-ray bands at 5.7 and 11 nm (Widom and Klug, 1985). Condensation correlates with the increase in the enthalpy of endotherm V, which reflects the denaturation of interacting core particles. Whether the different levels of folding of interphase chromatin (from the 30-nm fiber to heterochromatic domains) can be further distinguished using improved DSC methods remains an open question, however. Widom (1986) has recently shown that under appropriate ionic conditions chromatin fragments aggregate, forming coiled-coil or ropelike superstructures, within which individual 30-nm fibers are no longer discernible. An increase in the concentration of cations up to the precipitation point causes the x-ray diffraction bands to sharpen, suggesting that the solenoid undergoes a continuous folding process. Thus, from these experiments the picture emerges that the transition between the fully unfolded and condensed states cannot be considered an "all-or-none" transformation. The thermodynamic analysis of condensation leads to the same result; an intermediate endotherm at 100°C (V_b) has been related to the denaturation of partially folded domains (Cavazza et al., 1991).

The changes in chromatin structure associated with transformation share the major conformational features with the decondensation of chromatin in calf thymus nuclei at low ionic strength. However, important differences in the transition pattern are also apparent. In the case of the salt-dependent unfolding, the passage of transition enthalpy from V to IV obeys the kinetics of consecutive reactions; the intermediate state, corresponding to endotherm V_b, undergoes unfolding first (Cavazza et al., 1991). Decondensation in nodules, however, does not fully conform to this mechanism. The deconvolution of the excess heat capacity curve of early

nodules (Fig. 3 b) resolves endotherm V into the components V_b and V_a at 100 and 107°C. The comparison with the thermogram of nuclei from control hepatocytes (Fig. 3 a) shows that the conversion of condensed cromatin (transition V_a) into the looser structure that denatures in transition V_b is an early event in transformation. In fact, $\Delta H^{IV}{}_m$, $\Delta H^{Vb}{}_m$, and $\Delta H^{Va}{}_m$ correspond to 39, 38, and 23% of the total transition enthalpy, to be compared with 31, 29, and 40%, the values determined for control nuclei in the present experiment. That the more compact domains undergo unfolding right from the start cannot easily be explained according to simple physical models for decondensation, such as the increase in the electrostatic repulsion among nucleosomes.

Ultrastructure changes of chromatin in persistent nodules

Fig. 4 is a gallery of electron micrographs of thin sections of hepatocytes and nuclei from normal liver (a, c, and e) and hepatocytes from persistent (46-week) nodules (b, d, and f). The architecture of chromatin in control nuclei conforms to the well-established pattern typical of resting cells and needs no particular comment. Condensed chromatin is visible at the nuclear periphery as well as in the form of minor aggregates

FIGURE 3 Deconvolved excess heat capacity curves of nuclei isolated from control hepatocytes (a) and early developing (16-week) nodules (b). Note that endotherm V is resolved into two Gaussian components at 100°C (V_b) and 107°C (V_a).

scattered throughout the nucleoplasm. High-resolution micrographs (Fig. 5, a and b) show both 30-nm knobby fibers and thin filaments 10 nm in diameter. Within heterochromatic domains individual 30-nm fibers are no longer visible (Fig. 5 a). We note that the ultrastructure of chromatin found in intact hepatocytes survives the isolation of nuclei (compare Fig. 4, a and c, with Fig. 4 e), confirming the conclusion that our preparative protocol fully preserves the native configuration.

In persistent nodules the texture of chromatin undergoes a dramatic relaxation process. Heterochromatic domains are either completely absent (Fig. 4, b and d) or reduced to small aggregates with a beaded appearance (Fig. 4 f); in addition, the interchromatic areas contain a network of very thin fibrils. The fine details of this altered morphology can be seen in the high-resolution micrographs reported in Fig. 5 (c and d). Clusters or short alignments of 10-nm particles are the major structural motif of the loose chromatin network.

These observations are in remarkable agreement with the results of the DSC experiments, in that they show that the structural transition of chromatin occurring in nodules involves the unstacking of the core particles. To strengthen this conformational analogy with the unfolding induced by low-salt conditions, we show in Fig. 5 e the ultrastructure of a nucleus from normal liver decondensed in the presence of 10 mM Na$^+$, according to the procedure already described (Cavazza et al., 1991). In this sample, compared with the nodule shown in Fig. 5 d, the chromatin network shows less contrast, which may reflect the partial unfolding of the core particle at low ionic strength. Nevertheless, the path of the 10-nm fibrils and their distribution in the nucleoplasm are superimposable, as expected from the results of the DSC analysis, which shows directly that the interaction among nucleosomes is completely lost in persistent nodules.

DISCUSSION

Before we comment on the bearing of the extensive relaxation of chromatin on gene activation in transformed cells, a few remarks on the contention that the increase in the transition enthalpy at 90°C represents a physical marker of transformation are appropriate. It must be recalled that a similar drift in the thermal profile can be observed as a consequence of DNA chain scission, and we have already commented on the erratic correlations that can be established in the absence of an effective inhibition of endogenous nuclease activity (Balbi et al., 1989; Cavazza et al., 1991). The risk of artifacts is probably higher in nodules than in normal liver, as it has been shown that apoptosis (programmed cell death) appreciably contributes to the regulation of cell turnover during tumor development (Schulte-Hermann et al., 1988). We have found no evidence of the presence of appreciable amounts of extensively damaged DNA in our nuclear preparations. For example, the inset in Fig. 2 b shows a comparison between the electrophoretic patterns on 0.6% agarose gels of the DNA isolated from control hepatocytes (lane 1) and persistent nodules (lane 2). Although neither sample migrates significantly
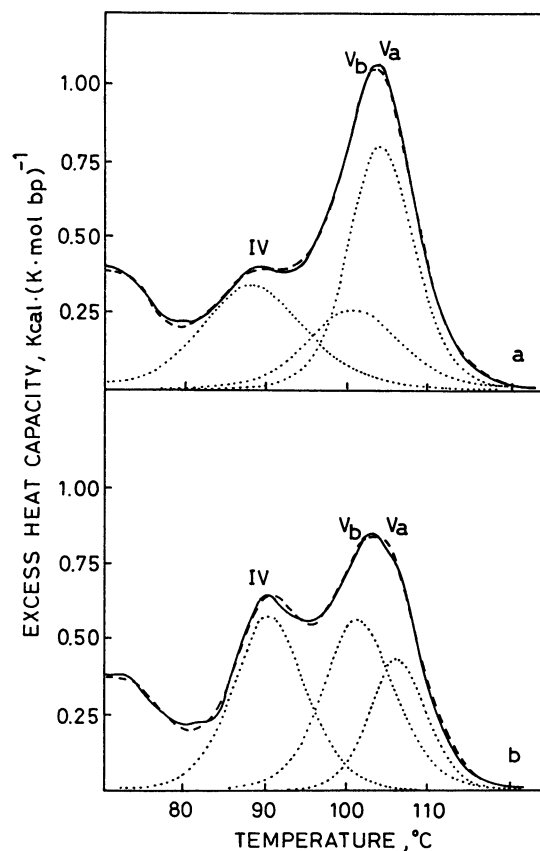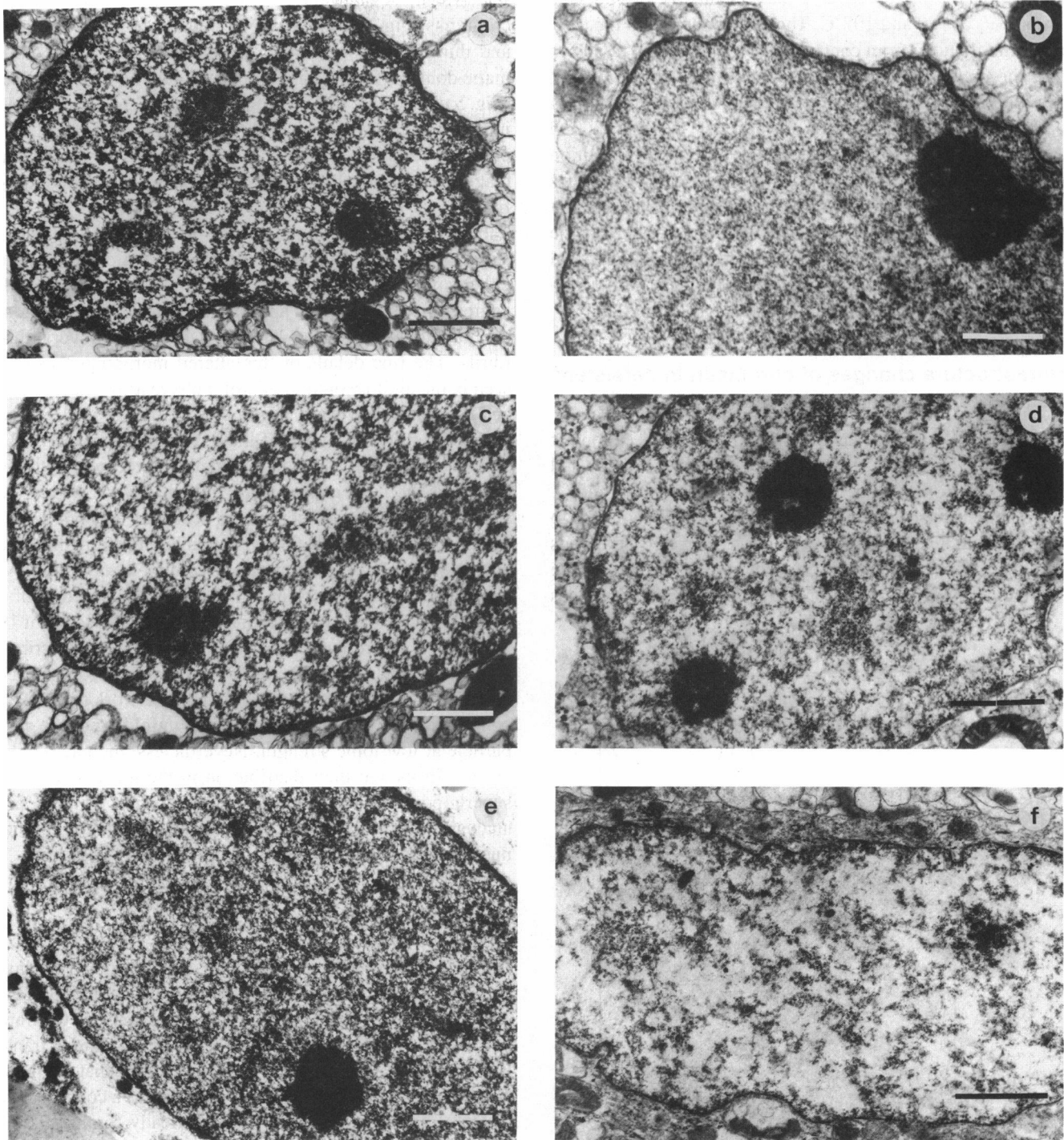
FIGURE 4   The morphology of nuclear chromatin in normal liver and persistent (46-week) nodules as visualized by electron microscopy of thin sections of isolated hepatocytes and nuclei. (a, c) control hepatocytes; (e) control nucleus; (b, d, f) hepatocytes from persistent nodules. The bar represents 1 μm.

through the gel, a small difference in the electrophoretic mobility can be appreciated; an approximate estimate of the most probable chain length yields a value of about 25 and 19 kilobase pairs for normal hepatocytes and persistent nodules, respectively. The latter value still turns out to be exceedingly high compared with the extensive degradation typical of the apoptotic cell, within which chromatin is cleaved to oligonucleosomal chains (Wyllie, 1980), and falls within the size

range expected for the DNA extracted with phenol-chloroform (10–30 kilobase pairs), a procedure that involves the degradation of the duplex by shearing forces, especially when precipitation with ethanol is employed (Maniatis et al., 1982). Moreover, previous digestion experiments of rat liver nuclei with micrococcal nuclease (Balbi et al., 1989) have shown that transition V disappears only when the most probable chain length of the DNA drops to 2 kilobase pairs.
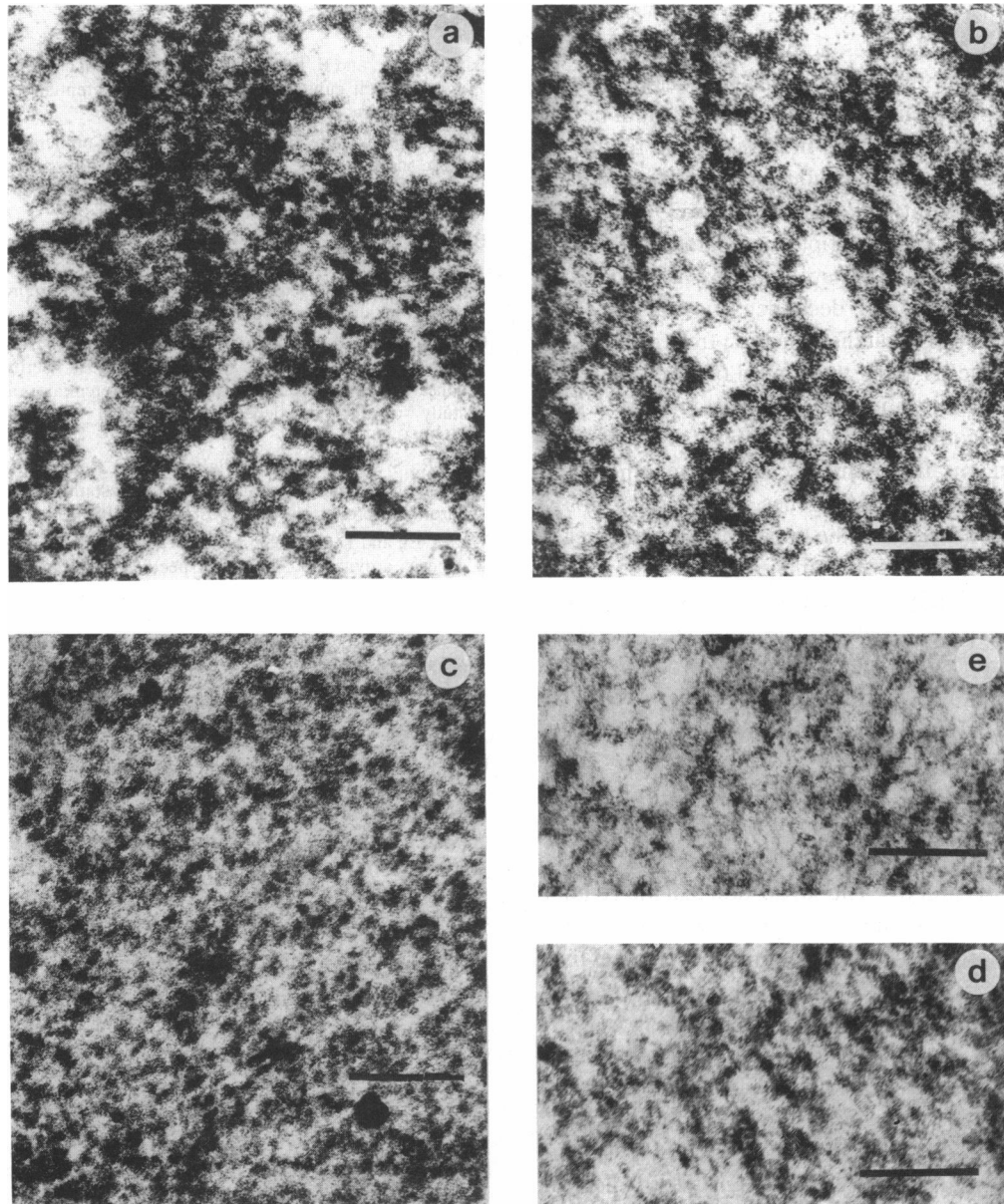
FIGURE 5   The ultrastructure of chromatin in normal liver (*a*, *b*) and persistent (46-week) nodules (*c*, *d*). (*e*) detail of a control nucleus incubated in dilute DM (Na$^+$ concentration, 10 mM) showing a loose network, shown for comparison. The bar represents 0.15 μm.

Since the unfolding of the higher-order structure is necessarily involved in DNA synthesis, the passage of denaturation enthalpy from transition V to IV could be related in nodules to the onset of proliferation. This explanation is inadequate, however. In persistent nodules the fraction of cells in S phase does not exceed 8% (Farber and Sarma, 1987). The thermal profile of nuclei from regenerating rat liver, isolated 20 h after partial hepatectomy, has been discussed in a previous paper (Balbi et al., 1989). Although in this case 30% of the hepatocytes traverse S, only a limited broadening of the 107°C endotherm was detected, a result consistent with the notion that the structure of chromatin is only transiently perturbed as replication proceeds. The same result is shown in Fig. 1 *a*, where the thermal profile of actively dividing TE

cells is compared with those of mature tissues. Extensive decondensation must therefore be regarded as a feature of transformation per se.

Significant structural differences between nodules and hepatocytes have been detected in the early stage of the transformation process. After deconvolution of the thermal profiles of early developing nodules into Gaussian components (Fig. 3 *b*) we find that the average degree of condensation is equal to 0.6, which is significantly lower than the value characteristic of the resting hepatocyte (0.7). Transformation in the resistant hepatocyte model involves a protracted sequence of phenotypic changes. Therefore, partial decondensation was expected on account of the onset of biochemical changes with respect to hepatocytes; the expression of sev-

eral enzymes that can activate xenobiotics decreases, whereas the level of enzymes active in detoxification increases. The complete relaxation of the higher-order structure occurring in persistent nodules, however, cannot be reconciled with simple mechanistic models for the regulatory function of heterochromatin. Although at this stage hepatocytes acquire the capacity to express a new 39-kDa cytokeratin (C. Balbi et al., manuscript in preparation), it is unclear why the synthesis of new proteins is temporally correlated with a catastrophic decondensation of the entire genome. We hypothesize that the transition from one cellular population to another is under the control of general cellular programs, which require most of the genes to be in a state of transcriptional competence. Of course, it might be objected that decondensation is merely an epiphenomenon of the primary activation of a few genes. The striking observation has also been made that the transformation of chicken embryo fibroblasts by Rous sarcoma virus results in the activation of an exceedingly large number of transcription units (Groudine and Weintraub, 1980). The only way to address this intriguing proposition and, hence, the problem of the regulatory function of heterochromatin is to further verify the occurrence of highly cooperative changes using different models for cell transformation.

Recent work from other laboratories (Feo et al., 1988; Leonardson and Levy, 1989; Laitinen et al., 1990), however, supports the notion that extensive chromatin unfolding is a primary event of the process. The suggestion that the genome is in a state of high transcriptional competence comes from a study on the pattern of hypomethylation of DNA in rat liver nodules (Feo et al., 1988). The content of 5-methyl-deoxycitidine decreases by about 50% with respect to normal liver; the hypomethylation sites are scattered throughout the genome. This large and apparently aspecific effect has a great deal in common with decondensation phenomena, since hypomethylation is correlated with both gene expression and cancer development. Its has been reported that newly derived Friend tumors show continuing changes in chromatin composition and nucleosome repeat length during early subcutaneous passages (Leonardson and Levy, 1989). In a thorough study of the nucleosomal organization of c-Ha-$ras^{Val\ 12}$ oncogene-transformed NIH-3T3 fibroblasts (Laitinen et al., 1990), Laitinen and his co-workers speculated that the degree of condensation of bulk chromatin plays a regulatory role in cell transformation. These findings, together with the observation on the physical state of chromatin reported in this work, stimulate the search for general modulating factors. Are histones and/or the nuclear matrix proteins involved? This question will be examined in detail in a later paper.

REFERENCES

Almagor, M., and R. D. Cole. 1989. Changes in chromatin structure during aging of cell cultures as revealed by differential scanning calorimetry Biochemistry. 28:5688–5693.

Balbi, C., M. L. Abelmoschi, A. Zunino, C. Cuniberti, B. Cavazza, P. Barboro, and E. Patrone. 1988. The decondensation process of nuclear chromatin as investigated by differential scanning calorimetry. Biochem. Pharmacol. 9:1815–1816.

Balbi, C., M. L. Abelmoschi, L. Gogioso, S. Parodi, P. Barboro, B. Cavazza, and E. Patrone. 1989. Structural domains and conformational changes in nuclear chromatin: a quantitative thermodynamic approach by differential scanning calorimetry. Biochemistry. 28:3220–3227.

Cavazza, B., G. Brizzolara, G. Lazzarini, E. Patrone, M. Piccardo, P. Barboro, S. Parodi, A. Pasini, and C. Balbi. 1991. Thermodynamics of condensation of nuclear chromatin. A differential scanning calorimetry study of the salt-dependent structural transitions. Biochemistry. 30:9060–9072.

Dorn, R., S. Heymann, L. Lindigkeit, and G. Reuter. 1986. Suppressor mutation of position-effect variegation in Drosophila melanogaster affecting chromatin properties. Chromosoma. 93:398–403.

Farber, E., and D. S. R. Sarma. 1987. Biology of disease. Hepatocarcinogenesis: a dynamic cellular perspective. Lab. Invest. 56:4–22.

Feo, F., R. Garcea, L. Daino, R. Pascale, S. Frassetto, P. Cozzolino, M. G. Vannini, M. E. Ruggiu, M. Simile, and M. Puddu. 1988. S-Adenosylmethionine antipromotion and antiprogression effect in hepatocarcinogenesis. Its association with inhibition of DNA methylation and gene expression. In Chemical Carcinogenesis. Models and Mechanisms. F. Feo, P. Pani, A. Columbano, and R. Garcea, editors. Plenum Press, New York and London. 407–423.

Franke, W. W., H. Denk, R. Kalt., and E. Schmid 1981. Biochemical and immunological identification of cytokeratin proteins present in hepatocytes of mammalian liver tissue. Exp. Cell Res. 131:299–318.

Frenster, J. H. 1974. Ultrastructure and function of heterochromatin and euchromatin. In The Cell Nucleus. H. Busch, editor. Academic Press, New York and London. 565–580.

Fulmer, A. W., and G. D. Fasman. 1979. Ionic strength-dependent conformational transitions of chromatin. Circular dichroism and thermal denaturation studies. Biopolymers. 18:2875–2891.

Groudine, M., and H. Weintraub. 1980. Activation of cellular genes by avian RNA tumor virus. Proc. Natl. Acad. Sci. USA. 77:5351–5354.

Laitinen, J., L. Sistonen, K. Alitalo, and E. Höltta. 1990. c-Ha-ras^{Val12} oncogene-transformed NIH-3T3 fibroblasts display more decondensed nucleosomal organization than normal fibroblasts. J. Cell Biol. 111:9–17.

Leonardson, K. E., and S. B. Levy. 1989. Chromatin reorganization during emergence of malignant Friend tumors: early changes in H2A and H2B variants and nucleosome repeat length. Exp. Cell Res. 180:209–219.

Maniatis, T., E. F. Fritsch, and J. Sambrook. 1982. Molecular Cloning: A Laboratory Manual. Cold Spring Harbor Laboratory, Cold Spring Harbor, NY.

Nicolini, C., V. Trefiletti, B. Cavazza, C. Cuniberti, E. Patrone, P. Carlo, and G. Brambilla. 1983. Quaternary and quinternary structures of native chromatin and DNA in liver nuclei: differential scanning calorimetry. Science (Washington DC). 219:176–178.

Olins, A. L., and D. E. Olins. 1979. Stereo electron microscopy of the 25-nm chromatin fibers in isolated nuclei. J. Cell Biol. 81:260–265.

Parodi, S., M. Pala, P. Russo, C. Balbi, M. L. Abelmoschi, M. Taningher, A. Zunino, L. Ottaggio, M. Deferrari, A. Carbone, and L. Santi. 1983. Alkaline DNA fragmentation, DNA disentanglement evaluated viscosimetrically and sister chromatid exchanges, after treatment in vivo with nitrofurantoin. Chem.-Biol. Interact. 45:77–94.

Reuter, G., M. Giarre, J. Farah, J. Gausz, A. Spiere, and P. Spierer. 1990. Dependence of position-effect variegation in Drosophila on dose of a gene encoding an unusual zinc-finger protein. Nature (Lond.). 344:219–223.

Schulte-Hermann, R., W. Bursch, L. Fesus, and B. Kraupp. 1988. Cell death by apoptosis in normal, preneoplastic and neoplastic tissue. In Chemical Carcinogenesis. Models and Mechanisms. F. Feo, P. Pani, A. Columbano, and R. Garcea, editors. Plenum Press, New York and London. 263–274.

Semple-Roberts, E., M. A. Hayes, D. Armstrong, R. A. Becker, W. J. Racz, and E. Farber. 1987. Alternative methods of selecting rat hepatocellular nodules resistant to 2-acetylaminofluorene. *Int. J. Cancer.* 40:643–645.

Solt, D., and E. Farber. 1976. New principle for the analysis of chemical carcinogenesis. *Nature (Lond.).* 263:701–703.

Staynov, D. Z. 1976. Thermal denaturation profiles and the structure of chromatin. *Nature (Lond.).* 264:522–525.

Svaren, J., and R. Chalkley. 1990. The structure and assembly of active chromatin. *Trends Genet.* 6:52–56.

Tokès, Z. A., and G. A. Clawson. 1989. Proteolytic activity associated with the nuclear scaffold. *J. Biol. Chem.* 264:15059–15065.

Touchette, N. A., and R. D. Cole. 1985. Differential scanning calorimetry of nuclei reveals the loss of major structural features in chromatin by brief nuclease treatment. *Proc. Natl. Acad. Sci. USA.* 82:2642–2646.

Touchette, N. A., E. Anton, and R. D. Cole. 1986. A higher order chromatin structure that is lost during differentiation of mouse neuroblastoma cells. *J. Biol. Chem.* 261:2185–2188.

Villeponteau, B., J. Brawley, and H. G. Martinson. 1992. Nucleosome spacing is compressed in active chromatin domains of chick erythroid cells. *Biochemistry.* 31:1554–1563.

Weintraub, H. 1985. Tissue-specific gene expression and chromatin structure. *Harvey Lect.* 79:217–244.

Weisbrod, S. 1982. Active chromatin. *Nature (Lond.).* 297:289–295.

Weischet, W. O., K. Tatchell, K. E. van Holde, and H. Klump. 1978. Thermal denaturation of nucleosomal core particles. *Nucleic Acids Res.* 5:139–160.

Widom, J. 1986. Physicochemical studies of the folding of the 100 Å nucleosome filament into the 300 Å filament. *J. Mol. Biol.* 190:411–424.

Widom, J., and A. Klug. 1985. Structure of the 300 Å chromatin filament. X-ray diffraction from oriented samples. *Cell.* 43:207–213.

Wyllie, A. H. 1980. Glucocorticoid-induced thymocyte apoptosis is associated with endogenous endonuclease activation. *Nature (Lond.).* 284:555–556.